JOC Article

Highly Nonplanar, Electron Deficient, N-Substituted tetra-Oxocyclohexadienylidene Porphyrinogens: Structural, Computational, and Electrochemical Investigations

Jonathan P. Hill,*,†,§ Ian J. Hewitt,† Christopher E. Anson,† Annie K. Powell,†
Amy Lea McCarty,‡ Paul A. Karr,‡ Melvin E. Zandler,‡ and Francis D'Souza*,‡

Institut für Anorganische Chemie, Universität Karlsruhe, Engesserstrasse 15, 76128 Karlsruhe, Germany, and Department of Chemistry, Wichita State University, 1845 Fairmount, Wichita, Kansas 67260-0051

hill@nanospace.miraikan.jst.go.jp; francis.dsouza@wichita.edu.

Received April 10, 2004

The structures and electrochemistry of N-benzylated *meso*-tetrakis (3,5-di-*tert*-butyl-4-oxo-cyclohexa-2,5-dienylidene) porphyrinogens have been investigated. Structural determinations reveal the isomeric identity of the products obtained from the N-alkylation of the parent *meso*-tetra (oxo-cyclohexadienylidene) porphyrinogen. The compounds are subject to increased macrocyclic deformations upon increasing N-substitution culminating in the tetra-*N*-benzyl derivative, which has a buckling superimposed on the already highly puckered macrocycle. The electrochemical analyses emphasize the electron deficiency of the N-benzylated *meso*-tetra(oxo-cyclohexadienylidene) porphyrinogens and indicate that they can be considered as quinones conjugated via the unsaturated tetrapyrrolic macrocycle. The N-benzylated compounds studied form stable and well-defined π-cation radical and π-anion radical species because of their highly conjugated nature. Ab initio molecular orbital calculations at the B3LYP/3-21G(*) level confirmed the high degree of conjugation between tetrapyrrole and meso substituents and also gave good agreement between calculated and experimentally determined HOMO−LUMO band gap energies.

Introduction

The tetrapyrrole macrocycles compose a class of compounds that are vital in biochemical systems.[1] In nature, they lie at the heart of many indispensable photo- and electrochemical assemblies.[2] Additionally, the synthetic porphyrins have become one of the most extensively studied classes of compounds not just because of their importance as model compounds for biological processes but as catalytic,[3] electronic,[4] and optical[5] materials. More recently, the field of porphyrin chemistry has been expanded by the use of imaginative synthetic procedures. Good examples of this are the higher cyclic oligopyrroles[6] and the development of porphyrin beta and meso substitution reactions.[7] Conventional porphyrinogens have also become an increasingly studied class of tetrapyrrole especially because of their rich synthetic and coordination chemistries[8] and for their potential as anion and cation binding agents.[9]

The phenol-substituted porphyrins as well as quinonoidal compounds derived from these have been characterized previously.[10] That work was aimed at investigating the relevance of the phenolic porphyrins to naturally occurring pigments and the redox processes in which they are involved. Although the redox chemistry of these

* Corresponding author. Phone: +81-3-3570-9181. Fax: +81-3-3570-9180.
† Universität Karlsruhe.
§ Current address: ERATO Nanospace Project, National Museum of Emerging Science and Innovation, 2-41, Aomi, Koto-ku, Tokyo 135-0064, Japan.
‡ Wichita State University.

(1) Milgrom, L. R. *The Colors of Life*; Oxford University Press: New York, 1997.
(2) (a) *The Porphyrin Handbook*; Kadish, K. M., Smith, K. M., Guilard, R., Eds.; Academic Press: Burlington, MA, 2000; Vol. 4. (b) Scheer, H. *Chlorophylls*; CRC Press: Boca Raton, FL, 1991. (c) Lewis, D. F. W. *Guide to Cytochromes P450*; Taylor and Francis: London, 2002.
(3) Bhyrappa, P.; Young, J. K.; Moore, J. S.; Suslick, K. S. *J. Am. Chem. Soc.* **1996**, *118*, 5708−5711 and references therein.
(4) For example: (a) Clausen, C.; Gryko, D. T.; Dabke, R. B.; Dontha, N.; Bocian, D. F.; Kuhr, W. G.; Lindsey, J. S. *J. Org. Chem.* **2000**, *65*, 7363−7370. (b) Li, J.; Gryko, D.; Dabke, R. B.; Diers, J. R.; Bocian, D. F.; Kuhr, W. G.; Lindsey, J. S. *J. Org. Chem.* **2000**, *65*, 7379−7390. (c) Suslick, K. S.; Rakow, N. A.; Kosal, M. E.; Chou, J.-H. *J. Porphyrins Phthalocyanines* **2000**, *4*, 407−413. (d) Morgado, J.; Cacialli, F.; Iqbal, R.; Moratti, S. C.; Holmes, A. B.; Yahioglu, G.; Milgrom, L. R.; Friend, R. H. *J. Mater. Chem.* **2001**, 11, 278−283. (e) Ambroise, A.; Wagner, R. W.; Rao, P. D.; Riggs, J. A.; Hascoat, P.; Diers, J. R.; Seth, J.; Lammi, R. K.; Bocian, D. F.; Holten, D.; Lindsey, J. S. *Chem. Mater.* **2001**, *13*, 1023−1034.
(5) For example: (a) Holten, D.; Bocian, D. F.; Lindsey, J. S. *Acc. Chem. Res.* **2002**, *35*, 57−69. (b) Screen, T. E. O.; Thorne, J. R. G.; Denning, R. G.; Bucknall, D. G.; Anderson, H. L. *J. Am. Chem. Soc.* **2002**, *124*, 9712. (c) Drain, C. M.; Hupp, J. T.; Suslick, K. S.; Wasielewski, M. R.; Chen, X. *J. Porphyrins Phthalocyanines* **2002**, *6*, 243−258.
(6) (a) Sessler, J. L.; Gebauer, A.; Weghorn, S. J. Expanded Porphyrins, in *The Porphyrin Handbook*; Kadish, K. M., Smith, K. M., Guilard, R., Eds.; Academic Press: Burlington, MA, 2000; Vol 2, Ch. 9. (b) Lash, T. D. *Angew. Chem., Int. Ed.* **2000**, *39*, 1763. (c) Setsune, J.; Maeda, S. J. *J. Am. Chem. Soc.* **2000**, *122*, 12405−12406. (d) Seidel, D.; Lynch, V.; Sessler, J. L. *Angew. Chem., Int. Ed.* **2002**, *41*, 1422−1425. (e) Srinivasan, A.; Ishizuka, T.; Osuka, A.; Furuta, H. *J. Am. Chem. Soc.* **2003**, *125*, 878−879.
(7) *The Porphyrin Handbook*; Kadish, K. M.; Smith, K. M.; Guilard, R., Eds.; Academic Press: Burlington, MA, 2000; Vol. 1.
(8) Floriani, C.; Floriani-Moro, R. *The Porphyrin Handbook*; Kadish, K. M.; Smith, K. M.; Guilard, R., Eds.; Academic Press: Burlington, MA, 2000; Vol. 3, Ch. 24 and 25.

10.1021/jo049401d CCC: $27.50
Published on Web 07/31/2004

compounds was studied, they represented somewhat of an impasse synthetically because of complex tautomeric mixtures and the formation of radical species when modification of the porphyrins was attempted.[11] However, the authors of those works were able to develop one synthetic system via the N-alkylation of the oxidized porphyrin derived from *meso*-tetrakis(3,5-di-*tert*-butyl-4-hydroxyphenyl) porphyrin.[12] This particular system was first brought to light by the unexpected N-alkylation of an unsymmetrically substituted tetraphenylporphyrin.[13] Having identified a viable route, several multiply N-substituted oxidized porphyrins were synthesized including some with nonidentical groups. In fact, up to three different nonidentical groups could be routinely introduced at the porphyrin nitrogen atoms making this system eminently suitable as a synthetic scaffold for synthesis of novel compounds.[14] In all previous studies, unambiguous characterization of the N-alkylated materials could not be claimed because of the lack of X-ray structural analyses and the resulting uncertainty over the isomeric identity of the N-alkylated compounds. Consequently, this promising system could not be exploited until structural data was forthcoming. We believed that the most significant aspect of these highly facially encumbered tetrapyrrolic compounds lies in the possibility of controlling their reduction toward the porphyrinic state. That is to say that one and two electron reductions to the radical and porphyrin state, respectively, allow access to metastable oxidation states. In fact, it has already been demonstrated that radical states of tetrapyrrolic compounds could be of use in volatile memory elements.[15] Furthermore, the variation of multiplicity and nature of N-substituents should allow us to tune the redox potentials of the reduction processes as desired. Under aerobic conditions, the reduced compounds spontaneously reoxidize to their native tetraoxocyclohexadienylidene porphyrinogen states presumably under steric influences.[16] Changes in oxidation state should also be associated with changes in the conformation of the tetrapyrrole and so the molecule, as a whole, will have an oxidation state-dependent shape. This has connotations for the application of derivatives of this type of compound in molecular sensing or information processing.[17,22]

We report herein on the structural, ab initio computational, electrochemical, and spectroelectrochemical characterization of some N-alkylated oxidized-porphyrin compounds. For the purposes of this study, we chose the most easily accessible N-alkylated compounds of an oxidized phenolic porphyrin. In this case, *meso*-tetrakis(3,5-di-*tert*-butyl-4-hydroxyphenyl) porphyrin, **1**, was selected because of the perceived ease of crystallization of its derivatives and because O-alkylation is somewhat hindered by the proximity of tertiary butyl groups to the phenol hydroxyl group. Oxidation of this porphyrin in basic solution gives the respective oxo-cyclohexadienylidene porphyrinogen, **2**,[18] whose structure has been reported.[19] Subsequent N-alkylation with benzyl bromide in refluxing ethanol in the presence of anhydrous potassium carbonate gives the required N-alkylated compounds in a varying ratio of yields depending on reaction time. Di- and tetra-substituted derivatives are consistently the major products, although some selectivity can be introduced by varying the nature of the substituting alkyl halide. It proved possible to isolate the mono- and trisubstituted derivatives, but the yields were low and they were usually neglected. Additionally, a very small degree of O-alkylation has been observed using more reactive benzyl bromides. The oxidation and N-alkylation can be achieved in one step, but a stepwise regime is preferred by us.

Results and Discussion

The chemical structures of the N-alkylated compounds are shown in Scheme 1. Two types of structural isomerism are possible in these materials. First, the exchangeable protons can be bound to phenolic oxygen or tetrapyrrole nitrogen atoms. Of course, this is not an issue in the fully N-substituted compound. The second type of isomerism concerns the relative position of the substituent benzyl groups and applies to both of the N-alkylated compounds. In **3**, the benzyl groups can be positioned on opposing or adjacent nitrogen atoms. The situation is further convoluted by the possibility of the benzyl groups occupying positions above or below the plane of the tetrapyrrole. Thus, for **3** and **4** there are four possible structural isomers (neglecting proton positional isomer-

(9) (a) Floriani, C.; Solari, E.; Solari, G.; Chiesi-Villa, A.; Rizzoli, C. *Angew. Chem., Int. Ed. Engl.* **1998**, *37*, 2245−2248. (b) Woods, C. J.; Camiolo, S.; Light, M. E.; Coles, S. J.; Hursthouse, M. B.; King, M. A.; Gale, P. A.; Essex, J. W. *J. Am. Chem. Soc.* **2002**, *124*, 8644−8652. (c) Sessler, J. L.; Camiolo, S.; Gale, P. A. *Coord. Chem. Rev.* **2003**, *240*, 17−55.

(10) (a) Milgrom, L. R. *Tetrahedron* **1983**, *39*, 3895−3898. (b) Albery, W. J.; Bartlett, P. N.; Jones, C. C.; Milgrom, L. R. *J. Chem. Res., Synopses* **1985**, *12*, 364−365. (c) Milgrom, L. R.; Mofidi, N.; Jones, C. C.; Harriman, A. *J. Chem. Soc., Perkin Trans.2* **1989**, 301−309. (d) Milgrom, L. R.; Mofidi, N.; Harriman, A. *J. Chem. Soc., Perkin Trans. 2* **1989**, 805−809. (e) Milgrom, L. R.; Mofidi, N.; Harriman, A. *Tetrahedron* **1989**, *45*, 7341−7352. (f) Milgrom, L. R.; Flitter, W. D.; Short, E. L. *J. Chem. Soc., Chem. Comm.* **1991**, 788−790. (g) Milgrom, L. R.; Hill, J. P. *J. Heterocyclic Chem.* **1993**, *30*, 1629−1633. (h) Milgrom, L. R.; Hill, J. P.; Flitter, W. D. *J. Chem. Soc., Perkin Trans. 2* **1994**, 521−524.

(11) Milgrom, L. R.; Yahioglu, G. *Free Radical Res.* **1996**, *24*, 19−29.

(12) Milgrom, L. R.; Hill, J. P.; Yahioglu, G. *J. Heterocycl. Chem.* **1995**, *32*, 97−101.

(13) Milgrom, L. R.; Hill, J. P.; Dempsey, P. F. *Tetrahedron* **1994**, *50*, 13477−13484.

(14) Hill, J. P. Ph.D. Thesis, Brunel University, U.K., 1995.

(15) Roth, K. M.; Yasseri, A. A.; Liu, Z.; Dabke, R. B.; Malinovskii, V.; Schweikart, K.-H.; Yu, L.; Tiznado, H.; Zaera, F.; Lindsey, J. S.; Kuhr, W. G.; Bocian, D. F. *J. Am. Chem. Soc.* **2003**, *125*, 505−517.

(16) The *N*-alkyl tetra-oxocyclohexadienylidene porphyrinogens were reduced under acidic conditions ($SnCl_2$/HCl(c)). The resulting porphyrin dications were stable until neutralization whereupon the starting N-alkylated tetra-oxocyclohexadienylidene porphyrinogens were obtained.[14]

(17) *Molecular Switches*; Feringa, B. L., Ed.; Wiley-VCH GmbH, Weinheim, 2001.

(18) Milgrom, L. R. *Tetrahedron* **1983**, *39*, 3895−3898.

(19) Golder, A. J.; Milgrom, L. R.; Nolan, K. B.; Povey, D. C. *J. Chem. Soc., Chem. Comm.* **1989**, 1751−1753.

(20) Structure figures of the unsubstituted parent, **2**, were generated from a CIF file obtained from the Cambridge Crystallographic Data Centre, 12 Union Rd., Cambridge, CB2 1EZ, UK. E-mail: data_request@ccdc.cam.ac.uk or fax: +44 1223 336033.

(21) Fleischer, E. B.; Stone, A. L. *J. Chem Soc., Chem. Commun.* **1967**, 332.

(22) (a) D'Souza, F.; Zandler, M. E.; Deviprasad, G. R.; Kutner, W. *J. Phys. Chem. A.* **2000**, *104*, 6887. (b) D'Souza, F.; Zandler, M. E.; Smith, P. M.; Deviprasad, G. R.; Arkady, K.; Fujitsuka, M.; Ito, O. *J. Phys. Chem. A* **2002**, *106*, 649. (c) Zandler, M. E.; Smith, P. M.; Fujitsuka, M.; Ito, O.; D'Souza, F. *J. Org. Chem.* **2002**, *67*, 9122. (d) Marczak, R.; Hoang, V. T.; Noworyta, K.; Zandler, M. E.; Kutner, W.; D'Souza, F. *J. Mater. Chem.* **2002**, *12*, 2123.

SCHEME 1

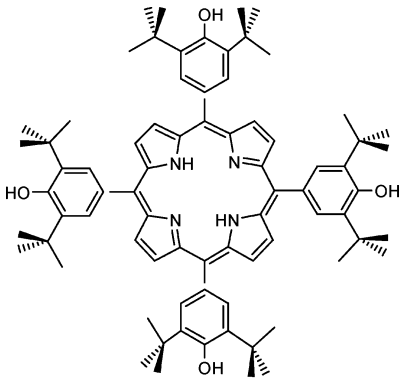

1

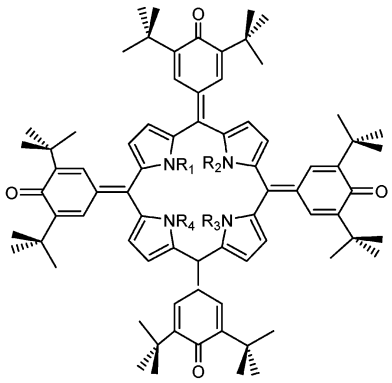

2: $R_1=R_2=R_3=R_4=H$
3: $R_1=R_3=H$; $R_2=R_4=CH_2C_6H_5$
4: $R_1=R_2=R_3=R_4=CH_2C_6H_5$

ism). Although the opposite over adjacent argument can be settled by use of ^1H NMR spectroscopy, the atropoisomerism of the N-alkyl groups cannot be conclusively determined by this method. Therefore, X-ray structural measurements were necessary to firmly establish the identity of these compounds. The structural studies reported here represent a significant advance for this class of compounds given the problems with obtaining single crystal diffraction data for more highly substituted derivatives.

Both di- and tetra-N-substituted derivatives were synthesized by careful control of reaction time and with monitoring by thin-layer chromatography. That the unevenly substituted derivatives are only available in low yield is noteworthy. This suggests an enhancement of reactivity of the mono- and tri-substituted derivatives toward N-alkylation, and therefore, that the reaction occurs in a strict stepwise manner since only single isomers of the two products have been so far isolated. The enhancement of reactivity is apparently regioselective with further substitution occurring only at an opposing nitrogen atom after mono-N-alkylation.

Figure 1 shows the optical absorption spectra of oxocyclohexadienylidene porphyrinogens along with the starting compound **1**. As expected for extended conjugated derivatives, the porphyrinogens **2**−**4** exhibited red-shifted absorption bands as compared to **1**. However, the bands were found to be broad with one or more shoulder bands instead of the usual Q-bands of porphyrins. The

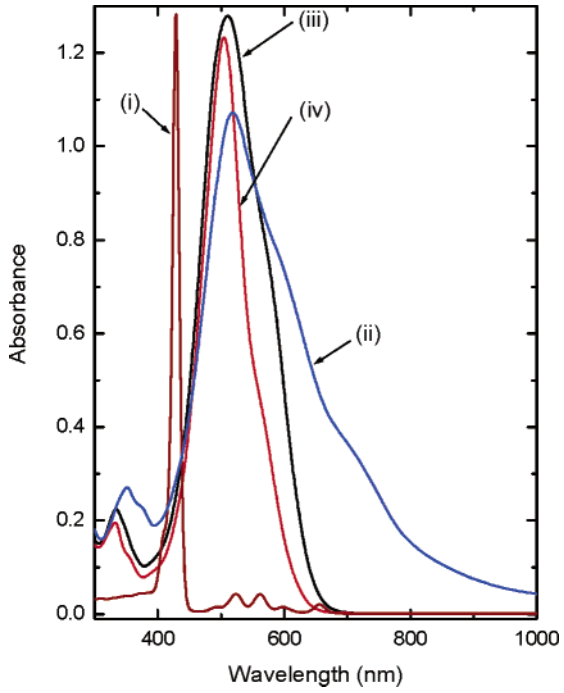

FIGURE 1. Optical absorption spectra of (i) *meso*-tetrakis-(3,5-di-*tert*-butyl-4-hydroxyphenyl)porphyrin (**1**), (ii) tetrakis-(3,5-di-*tert*-butyl-4-oxo-cyclohexa-2,5-dienylidene)porphyrinogen (**2**), (iii) N_{21},N_{23}-dibenzyl-5,10,15,20-(3,5-di-*tert*-butyl-4-oxo-cyclohexa-2,5-dienylidene)porphyrinogen (**3**), and (iv) N_{21},N_{22},N_{23},N_{24}-tetrabenzyl-5,10,15,20-(3,5-di-*tert*-butyl-4-oxo-cyclohexa-2,5-dienylidene)porphyrinogen (**4**) in 1,2-dichlorobenzene.

absorption maxima of the Soret-type band were located at 518, 509, and 504 nm for **2**, **3**, and **4**, respectively. That is, upon N-substitution, the porphyrinogens exhibited a small blue shift in their absorption maxima.

Crystals of **3** and **4** were grown by slow evaporation of toluene and hexane solutions, respectively. The intensely violet or red solutions yield olive green crystals for reasons probably related to crystal packing rather than to tautomerism involving exchangeable protons since this situation is also true for the tetra-N-alkylated derivatives where no exchangeable protons are available for such tautomerism. However, solvatochromic effects can also be considered and are under investigation by us. There are several important features in the structure of **3**. First, and most obviously, the benzyl groups are substituted at the central nitrogen atoms without changing the overall conformation of the macrocycle relative to the unsubstituted material.[19] Additionally, an analysis of the meso substituent C−O bonds indicates that they are all double bonds (ca. 1.24 Å), revealing that the two remaining exchangeable protons reside at the central nitrogen atoms. This is further confirmed in the structure by the presence of a water molecule that is strongly hydrogen bonded via these N−H protons ($N_{pyrrole}$−O_{water} 3.02 Å) and the N−H resonance at low field in the proton NMR spectrum of **3**. Further bond length analyses confirm that the meso substituents are 4-oxo-cyclohexa-2,5-diene moieties and that these are bonded at the meso positions via double bonds. The meso substituents can similarly be assigned as 4-oxo-cyclohexa-2,5-dienes in **4**.

A comparative illustration of the three related structures is given in Figure 2 (the structure of the nonalky-

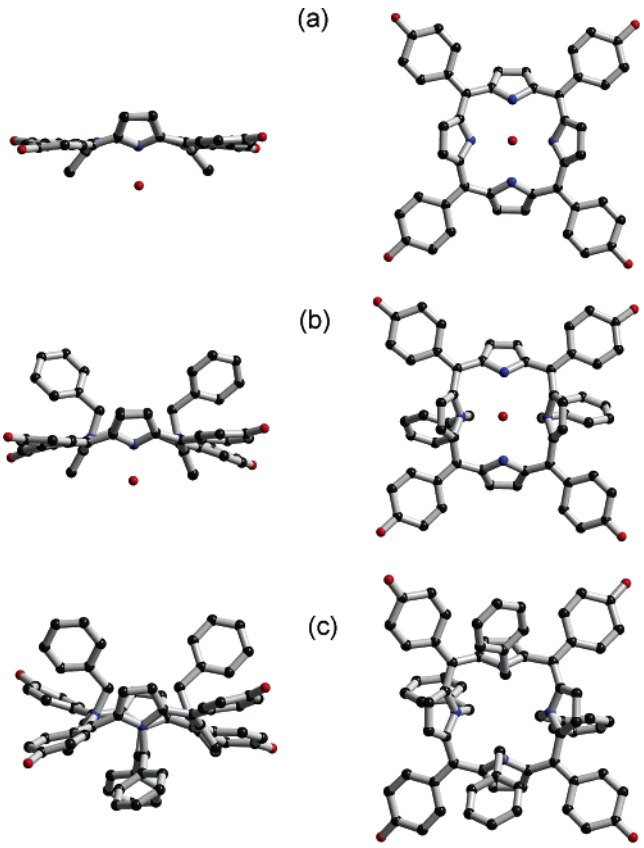

FIGURE 2. Comparison of the skeletal deformations upon N-alkylation in the X-ray crystal structures of (a) **2**[20], (b) **3**, and (c) **4**.

lated material was reported previously[19]). The crystal packing of **2** is strongly influenced by the waters of crystallization. There is extensive H-bonding, which results in the formation of a layered structure. Substitution at the central nitrogen atoms effectively disrupts the formation of any networked structure and allows binding of a discrete water guest molecule by hydrogen bonding between tetrapyrrole N−H and the water oxygen atom. Crystal packing of the N-alkylated oxidized porphyrin derivatives is not characterized by any important interactions. There are no short contact distances, and hydrogen bonding or other special packing forces are not apparent. Therefore, the comparative discussion is restricted to the molecular stuctures of the species, **2**, **3**, and **4**. For this purpose, Figure 2 illustrates the skeletal deformations that occur upon increasing substitution of **2** by benzyl groups.

The most notable effect of introducing bulky substituents at the nitrogen atoms is the increased distortion of the porphyrinogen framework. Thus, while in **2** there is an even and alternating deviation of 48° by all the pyrrole rings away from the least squares plane of the macrocycle, the noncoplanarity in **3** is marked by an uneven puckering where the unalkylated pyrroles have dihedral angles slightly larger than **2** but the substituted pyrrole rings have a deviation from the mean plane of 60.84 and 67.99°. The unsubstituted pyrroles are involved in hydrogen bonding with a molecule of water, which probably stabilizes the macrocycle in this particular conformation.

Further N-substitution does not, however, lead to an extension of the puckering. Rather, the conflicting driving forces of steric hindrance and π-conjugation conspire to produce a highly distorted structure in which the pyrrole groups are allowed to occupy a less puckered conformation. In **4**, the average dihedral angle subtended by the pyrrole rings and the macrocyclic plane is around 53°. In the cases of **2** and **3**, the changes in electronic structure and steric constraints caused by oxidation and N-substitution, respectively, can be accommodated by a simple out-of-plane hinging of the pyrrole groups. However, in **4**, the presence of two extra benzyl groups requires an additional torsional distortion over the entire macrocycle, although this is also evident to some extent in **3**. In the absence of an X-ray structure for **1**, a computed structure was used for comparative purposes. The computed structure gave a dihedral angle of 0.04°, indicating an almost planar porphyrin macrocycle (see Supporting Information). The dication of **1**, $[T(DtBHP)PH_4]^{2+}$, is likely to have a dihedral angle close to 33°, which is the value obtained experimentally for the dication of unsubstituted *meso*-tetraphenylporphyrin.[21] Table 2 contains the displacement distances of the macrocyclic atoms from the macrocyclic mean plane. These values confirm the distortion suffered by the macrocycle upon N-substitution and further illustrate the hinging of the pyrrole groups in **3** and the reduction in puckering upon complete N-substitution. The β-carbon atoms of N-substituted pyrrole rings in **3** are displaced by an average of 1.63 Å, while this value is reduced to 1.39 Å in **4**.

TABLE 1. Ab Initio B3LYP/3-21G(*) Calculated Parameters for the Investigated Porphyrin and Porphyrinogens

compound	HOMO+1 eV	HOMO, eV	LUMO, eV	LUMO+1, eV	HOMO−LUMO gap eV
T(DtBHP)P, **1**	−5.147	−4.711	−2.029	−2.017	2.68
Ox[T(DtBHP)P], **2**	−5.831	−5.536	−3.624	−3.060	1.91
Ox[T(DtBHP)P]Bz_2, **3**	−5.754	−5.515	−3.501	−3.089	2.01
Ox[T(DtBHP)P]Bz_4, **4**	−5.826	−5.464	−3.420	−2.941	2.04

TABLE 2. Electrochemical Redox Potentials (V vs Fc/Fc^+) of the N-Substituted tetra-oxo-Cyclohexa-2,5-dienylidene Porphyrinogens in *o*-Dichlorobenzene, 0.1 M (TBA)ClO_4[a]

compound	second ox.	first ox.	first red.	second red.	third red.	fourth red.
T(DtBHP)P, **1**	0.43[b]	0.31[b]	−1.82	−2.19		
Ox[T(DtBHP)P], **2**	0.48	0.27	−1.33[c]			
Ox[T(DtBHP)P]Bz_2, **3**	0.69	0.48	−1.38[c]	−1.45	−2.00	−2.08
Ox[T(DtBHP)P]Bz_4, **4**		0.73[b]	−1.34[c]	−1.38	−1.86	

[a] Scan rate = 100 mV/s. [b] E_{pa} at 0.1 V/s. [c] E_{pc} at 0.1 V/s.

During these changes in macrocyclic structure, there is also a perturbation in the conformation of the meso substituents. These are essentially coplanar with each other in **2**, while in **3** there is a somewhat uneven but slight departure from coplanarity that may be due, in part, to crystal packing forces. The situation for **4**, however, reflects again the steric perturbation that the four benzyl substituents exert in this compound. The meso groups are themselves arranged in a puckered manner with groups in opposing meso positions (i.e., 5 and 15; 10 and 20) deviating in the same direction, as can be seen in Figure 2c.

In conclusion, it is interesting to observe the effect of increasing substitution at the central nitrogen atoms of **2** especially in view of the highly conjugated nature of these compounds. Changes in conformation of the pyrrole rings must also allow a maximum conjugative overlap between the component macrocycle and meso substituent orbitals. Therefore, although the introduction of two benzyl groups at opposing nitrogen atoms introduces a significant steric crowding, there is only a localized distortion resulting in the increased angle between N-substituted pyrrole and macrocyclic mean plane. Conversely, if all nitrogen atoms are N-substituted with benzyl groups, the molecule is more distorted with both macrocycle and meso substituents taking up a puckered structure. It should be noted that the crystal structures of **3** and **4** are not governed by any strong intermolecular forces, so that packing constraints become more significant as compared to other interactions especially in these compounds that contain multiple tertiary butyl substituents. Thus, a less distorted conformation (i.e., that represented by the calculated structure) is likely to exist in solution.

Ab Initio B3LYP/3-21G(*) Computational Studies. To gain insight into their geometry and electronic structure, computational studies were performed on compounds **1**−**4** by using density functional methods (DFT) at the B3LYP/3-21G(*) level. The DFT methods were chosen over the Hartree−Fock or semiempirical approach since recent studies on porphyrin−fullerene dyads and ferrocene−fullerene−nitroaromatic triads have shown that the DFT methods at the 3-21G(*) level predict the geometry and electronic structure much more accurately.[22]

In our calculations, all of the compounds were fully optimized to a stationary point on the Born−Oppenheimer potential energy surface. To gain more confidence in the computed structures, especially the nonplanarity factors, the computed structures were compared with the X-ray structures. The results of the comparison are depicted in the flat-scale projections shown in Figure 3. The flat-scale projections were generated by least-squares fitting a plane to the 24 heavy atoms of the porphyrin ring, establishing the origin of the plane at the centroid of the 24 atoms, defining the positive *X*-axis in the direction of one of the meso carbons, the positive *Y*-axis orthogonal to *X* in the direction of another one of the meso carbons, and the positive *Z*-axis orthogonal to the *XY* plane. The original atomic coordinates were transformed to the newly defined coordinate system, and the *Z*-coordinate was plotted against the angle of the arctangent of the *XY* coordinates. For compound **2**, bearing no N-substituents, an excellent agreement between computed and X-ray structure was observed. Here, the β-pyrrole carbons were displaced as much as 1.7 Å from the least squares plane. The nonplanarity of the porphyrinogen macrocycle is comparable to that reported previously for highly substituted porphyrins.[23] Additionally, it is interesting to note that the X-ray and computed structures are very similar, suggesting that the extensive

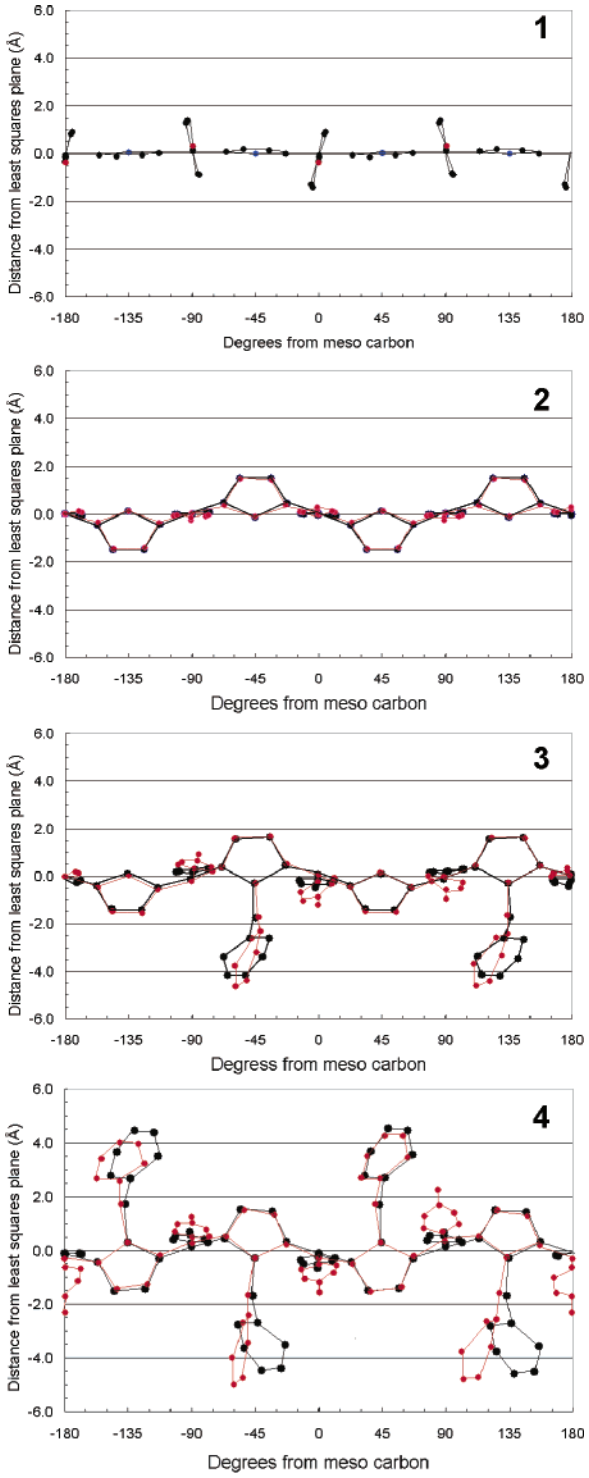

FIGURE 3. Plots of the edge-on view of the porphyrin ring atoms plotted by vertical distance from the least squares plane of the 20 porphyrin atoms for both calculated (black line) and X-ray (red line) structures.

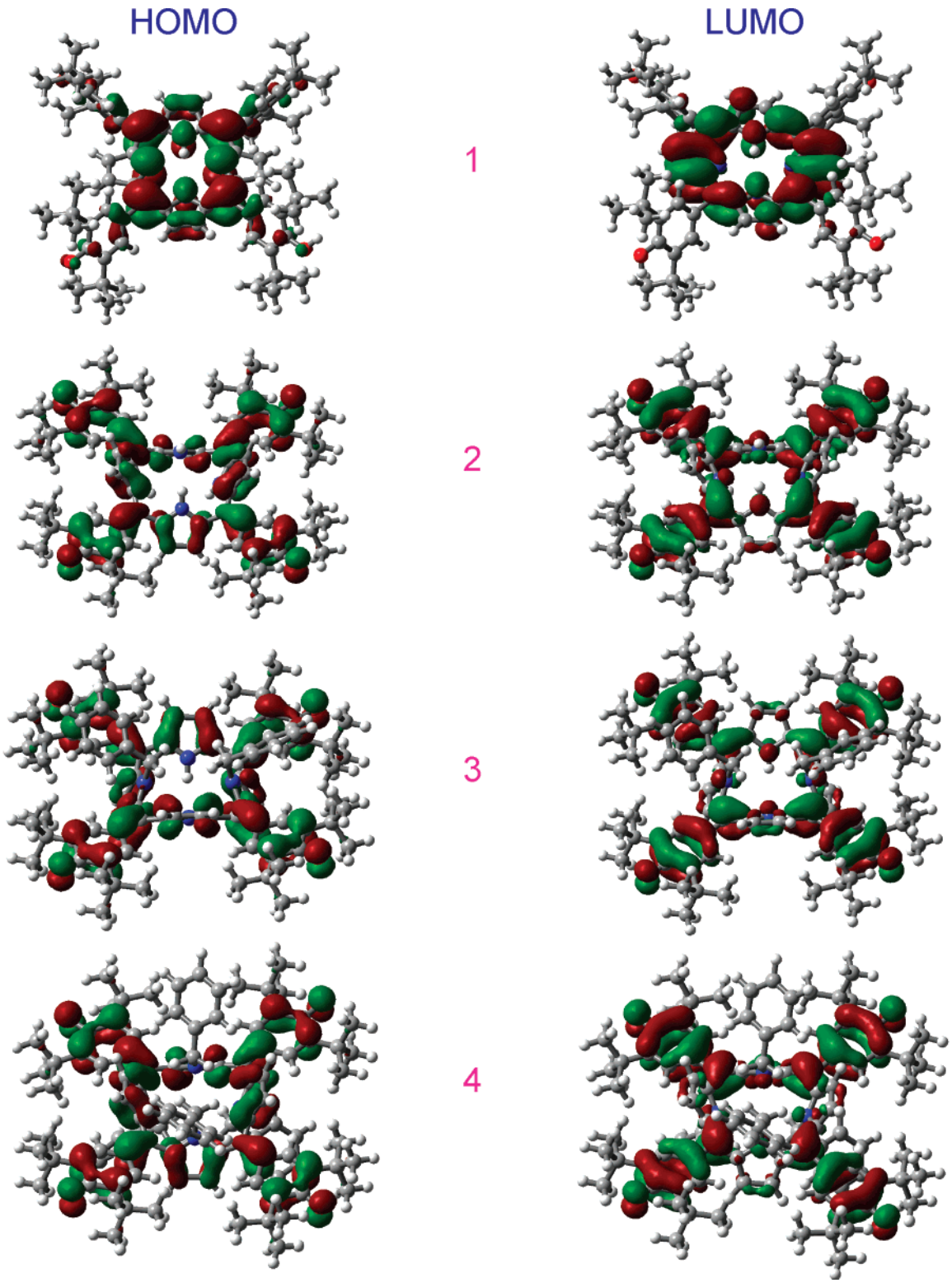

FIGURE 4. Coefficients of the first HOMO and the first LUMO for the B3LYP/321G(*) optimized *meso*-tetrakis(3,5-di-*tert*-butyl-4-hydroxyphenyl)porphyrin (**1**), tetrakis(3,5-di-*tert*-butyl-4-oxo-cyclohexa-2,5-dienylidene)porphyrinogen (**2**), N_{21},N_{23}–dibenzyl-5,-10,15,20-(3,5-di-*tert*-butyl-4-oxo-cyclohexa-2,5-dienylidene)porphyrinogen (**3**), and N_{21},N_{22},N_{23},N_{24}-tetrabenzyl-5,10,15,20-(3,5-di-*tert*-butyl-4-oxo-cyclohexa-2,5-dienylidene) porphyrinogen (**4**).

H-bonding in the crystals of **2** has little effect on its molecular conformation.

Compounds **3** and **4**, bearing two and four N-benzyl substituents, respectively, exhibited macrocyclic distortions similar to compound **2** (i.e., the β-pyrrole carbons were displaced by around 1.7 Å). The position of the N-substituted benzyl groups could not exactly be matched with the X-ray structure since crystal packing makes these flexible substituents occupy less symmetric positions. However, the excellent agreement of the porphyrin

ring atoms between the computed and the X-ray structures gave us enough confidence to investigate the electronic structure of these molecules.

Figure 4 illustrates the first HOMO and first LUMO of compounds **1**−**4**, while Table 1 lists the energies of the first two HOMOs and first two LUMOs along with the calculated HOMO−LUMO gap. As expected for porphyrins, the HOMOs and LUMOs of compounds **1**−**4** were all π-orbitals. However, the symmetries of the HOMO orbitals of compounds **2**−**4** were different (pseudo-D_{2d}, a_2 HOMO, and b_2 LUMO) from compound **1** (pseudo-D_{4h}, a_{1u}, a_{2u} HOMO, and e_g LUMO). The HOMO and LUMO orbitals for compound **1** were found to be mainly on the porphyrin π-ring system, while for **2**−**4** these orbitals were spread to the oxo-cyclohexadienylidene rings of the porphyrinogen macrocycle due to the extension of conjugation caused by oxidation. Interestingly, there are only minor orbital contributions on the ring nitrogens (only for the LUMO), and almost no contribution from the benzyl groups was observed. The calculated HOMO−LUMO gap followed the trend **2** < **3** < **4** < **1**. These results suggest a decreased HOMO−LUMO gap for the porphyrinogens as compared to the parent porphyrin, and this gap increases slightly with increasing number of N-substituents at the porphyrinogen macrocycle.

Electrochemical Studies. Electrochemical studies were performed to evaluate the redox potentials and to verify the predictions of computational studies on the HOMO−LUMO gap. Comparison between the experimental results and that predicted by theory has been of general interest for both experimental and theoretical chemists not only to check the validity of their procedures but also to design molecular systems with novel physicochemical properties.[24] In our studies, dry 1,2-dichlorobenzene, freshly distilled over CaH_2, was used to prevent proton-coupled chemical reactions that might occur upon electrochemical oxidation and reduction of the investigated compounds. Dried, recrystallized samples were used for the electrochemical studies. Figure 5 shows the cyclic voltammograms of the three porphyrinogens along with the starting material, *meso*-tetrakis(3,5-di-*tert*-butyl-4-hydroxyphenyl) porphyrin, **1**, while Table 2 lists the values of the redox potentials. The cyclic voltammogram of tetra-oxo-cyclohexadienylidene porphyrinogen, **2**, bearing no N-substitutents, revealed two reversible oxidations located at $E_{1/2}$ = 0.27 and 0.48 V versus Fc/Fc$^+$ and an irreversible reduction at E_{pc} = −1.33 V versus Fc/Fc$^+$. The larger current for this reduction process suggests the involvement of one or more electrons. Variable scan rate, multicyclic, and low-temperature (0 °C) voltammetric studies revealed no changes in the shape of the voltammogram. Interestingly, compounds **3** and **4** exhibited a systematic anodic shift in their oxidation potentials. The first oxidations of **3** and **4** (quasireversible) are located at $E_{1/2}$ = 0.48 and E_{pa} = 0.73 V versus Fc/Fc$^+$. These values represent over 200 and 400 mV shifts in their oxidation potentials, respectively.

A similar but less pronounced trend was observed during the reduction of the oxo-cyclohexadienylidene porphyrinogens. While the reduction of **2** was fully

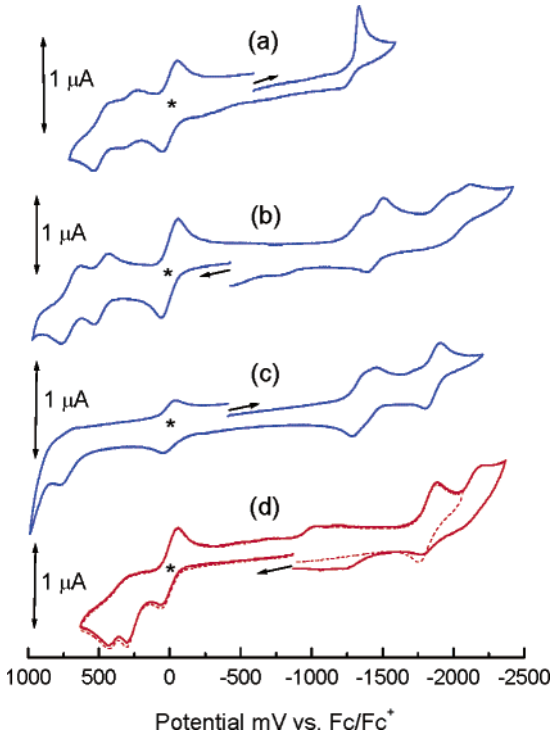

FIGURE 5. Cyclic voltammograms of (a) tetrakis (3,5-di-*tert*-butyl-4-oxo-cyclohexa-2,5-dienylidene) porphyrinogen, (b) N_{21},N_{23}–dibenzyl-5,10,15,20-(3,5-di-*tert*-butyl-4-oxo-cyclohexa-2,5-dienylidene) porphyrinogen, (c) N_{21},N_{22},N_{23},N_{24}-tetrabenzyl-5,10,15,20-(3,5-di-*tert*-butyl-4-oxo-cyclohexa-2,5-dienyl idene)-porphyrinogen, and (d) *meso*-tetrakis(3,5-di-*tert*-butyl-4-hydroxyphenyl)porphyrin in 1,2-dichlorobenzene, 0.1 M (TBA)ClO_4. Scan rate = 100 mV/s. The asterisk indicates the Fc/Fc$^+$ redox couple used as an internal standard.

irreversible, the cyclic voltammograms corresponding to the reduction of **3** and **4** were found to be quasireversible to reversible. Scanning the potential to more negative values revealed additional reductions (Figure 5) for **3** and **4**. The potentials corresponding to the first reduction of compounds **2**−**4** were found to be close to each other (Table 2). The cyclic voltammogram of **1** revealed two irreversible oxidation peaks located at E_{pa} = 0.31 and 0.43 V versus Fc/Fc$^+$, and as expected for free-base porphyrins, two reversible reductions at $E_{1/2}$ = −1.82 and −2.19 V versus Fc/ Fc$^+$. The location and irreversible nature of the anodic waves suggest oxidation of the porphyrin ring leading to the formation of oxo-cyclohexadienylidene porphyrinogens. It is important to note that the oxidation behavior of **1** and the reduction behavior of **2** complement each other, that is, the irreversible reduction of **2** involves the conversion of oxo-cyclohexadienylidene porphyrinogens to the tetrakis(4-hydroxyphenyl)porphyrin (in its deprotonated form in the absence of protons). Importantly, the magnitude of the redox potentials of compounds **2**−**4** suggests that these compounds are electron deficient. That is to say that they are nearly 500 mV easier to reduce than **1**.

The HOMO−LUMO gaps calculated from computational studies and from the electrochemical measure-

(23) Shelnutt, J. A.; Song, X.-Z.; Ma, J.-G.; Jia, S.-L.; Jentzen, W.; Medforth, C. J. *Chem. Soc. Rev.* **1998**, *27*, 31 and references therein.

(24) Langford, S. J.; Yann, T. *J. Am. Chem. Soc.* **2003**, *125*, 11198. (b) *Introduction to Molecular Electronics*; Petty, M. C.; Bryce, M. R.; Bloor, D., Eds.; Oxford University Press: New York, 1995.

TABLE 3. Comparison between the HOMO−LUMO Gap Calculated from Electrochemical and Computational (B3LYP/3-21G(*)) Methods

compound	electrochemical, V	computational, eV
T(DtBHP)P, **1**	2.13	2.68
Ox[T(DtBHP)P], **2**	1.60	1.91
Ox[T(DtBHP)P]Bz_2, **3**	1.86	2.01
Ox[T(DtBHP)P]Bz_4, **4**	2.07	2.04

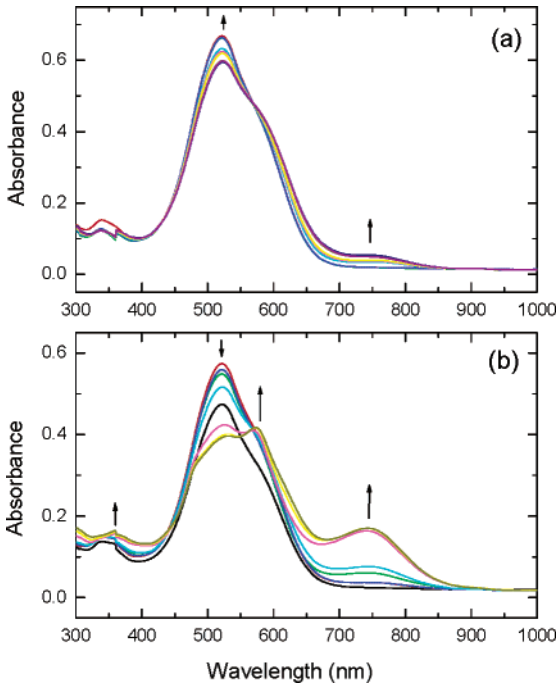

FIGURE 6. Spectral changes observed during (a) first oxidation and (b) first reduction of N_{21},N_{23}–dibenzyl-5,10,15,20-(3,5-di-*tert*-butyl-4-oxo-cyclohexa-2,5-dienylidene) porphyrinogen in *o*-dichlorobenzene, 0.1 M (TBA)ClO_4.

ments (the difference between first oxidation and first reduction potentials) are listed in Table 3. For the trend of the HOMO−LUMO gap, **2** < **3** < **4** < **1,** excellent agreement between computed and experimental results is observed. These observations are also consistent with the optical absorption data shown in Figure 1, where the position of the absorption bands also follows a similar trend. Previously, similar attempts have been made to match the HOMO−LUMO gap from computational, electrochemical, and optical studies.[25] The results presented here serve as an excellent illustration that this is an attainable goal.

The anodic shift and reversibility of the oxidation processes clearly suggest stabilization of the HOMO of tetra-oxo-cyclohexadienylidene porphyrinogens upon N-substitution. Although the effect on the LUMO is less, the reductions of **3** and **4** are reversible as compared to the irreversible reduction of **2**. The reversible redox processes of **3** and **4** suggest formation of stable π-cation and π-anion radicals upon the first oxidation and first reduction processes. Spectral characterization of such radicals is essential considering the extended π-conjugation of the tetra-oxo-cyclohexadienylidene porphyrinogen macrocycles and their possible applications as materials for building molecular electronic devices[24] or electron-transfer model compounds.[26] With this in mind, we have performed spectroelectrochemical characterization of the oxidized and reduced species of **3** and **4**, and the results are discussed next.

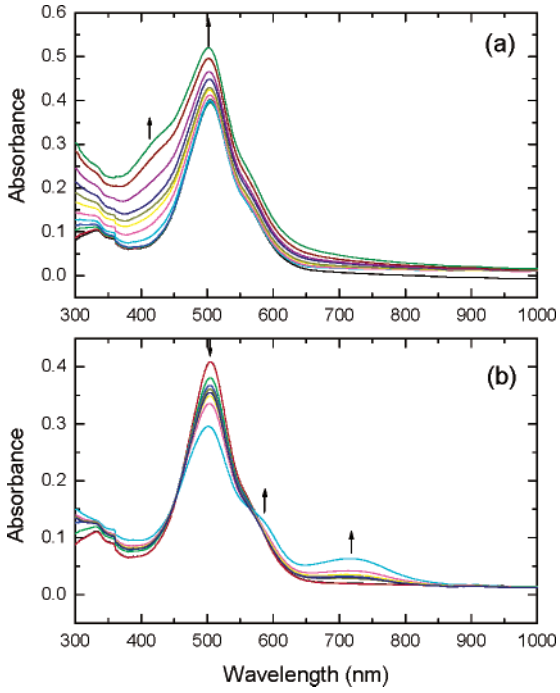

FIGURE 7. Spectral changes observed during (a) first oxidation and (b) first reduction of N_{21},N_{22},N_{23},N_{24}-tetrabenzyl-5,-10,15,20-(3,5-di-*tert*-butyl-4-oxo-cyclohexa-2,5-dienylidene)-porphyrinogen in *o*-dichlorobenzene, 0.1 M (TBA)ClO_4.

Spectroelectrochemical Studies. Figures 6 and 7 present the spectral changes observed during the oxidation and reduction of **3** and **4**, respectively, in *o*-dichlorobenzene containing 0.1 M (TBA)ClO_4. The spectral changes recorded during the first oxidation of **3** revealed new absorption bands at 588 and 750 nm with a decrease in the Soret band intensity (Figure 6a).

Isosbestic points at 430 and 570 nm were also observed, suggesting the occurrence of only one equilibrium process in solution. Similar observations were also made during the first reduction of **3**. New absorption bands at 744 and 572 nm were observed with a concurrent decrease of the Soret band intensity of the neutral species. No new spectral bands were observed during the oxidation of **4** with the spectra undergoing only a small intensity gain (Figure 7). Interestingly, the reduction of **4** resulted in the formation of well-resolved bands at 571 and 589 nm with a concurrent decrease of the Soret band at 504 nm. Isosbestic points were also observed at 454 and 571 nm.

The observation of the nicely formed π-cation radical spectra, and especially the π-anion radical spectra of **3** and **4**, clearly suggest their higher stability as predicted

(25) (a) Ghosh, A. *Acc. Chem. Res.* **1998**, *31*, 189. (b) Ghosh, A. *J. Am. Chem. Soc.* **1995**, *117*, 4691. (c) Ghosh, A. *J. Phys. Chem.* **1994**, *98*, 11004. (d) D'Souza, F.; Zandler M. E.; Tagliatesta, P.; Ou, Z., Shao, J., Caemelbecke, E. V., Kadish, K. M. *Inorg. Chem.* **1998**, *37*, 4567.

(26) (a) Sutin, N. *Acc. Chem. Res.* **1983**, *15*, 275. (b) Wasielewski, M. R. *Chem. Rev.* **1992**, *92*, 435. (c) Gust, D.; Moore, T. A.; Moore, A. L. *Acc. Chem. Res.* **1993**, *26*, 198. (d) Paddon-Row: M. N. *Acc. Chem. Res.* **1994**, *27*, 18. (e) Hayashi, T.; Ogoshi, H. *Chem. Soc. Rev.* **1997**, *26*, 355. (f) Piotrowiak, P. *Chem. Soc. Rev.* **1999**, *28*, 143. (g) Guldi, D. M. *Chem. Soc. Rev.* **2002**, *31*, 22.

from the reversible redox processes. It should be mentioned here that spectroelectrochemical investigations of the oxo-cyclohexadienylidene porphyrinogen derivative without N-substitution, **2**, revealed irreversible spectral features without the presence of clear isosbestic points. The present electrochemical and spectroelectrochemical studies collectively indicate that the investigated tetra-oxo-cyclohexadienylidene porphyrinogens are electron deficient and become stable toward the formation of cation and anion species upon N-substitution.

Conclusion

We have presented the structural and electrochemical characterization of an interesting class of N-alkylated tetrapyrrole macrocycles. The N-alkylation has been shown to occur at the pyrrolic nitrogen atoms without altering the conformation of the macrocycle. This is a significant point since it allows us to predict the three-dimensional structure of other similar derivatives where structural data is not available. Moreover, this system avoids the purported difficulties of tautomerism in phenolic porphyrin systems while retaining the possibility of porphyrinic cation radical states that are available through electrolytic or chemical reductions. The X-ray structural analyses along with the ab initio computational studies revealed highly nonplanar macrocycles in compounds **3** and **4**. The electrochemical studies revealed that the porphyrinogen ring is electron deficient by nearly 500 mV and that the redox processes of N-substituted **3** and **4** are better defined than those of **2**. The computationally predicted and electrochemically determined HOMO−LUMO gap followed the trend **2** < **3** < **4** < **1**. As predicted from the electrochemical studies, spectroelectrochemical studies confirmed stable π-cation and π-anion radical formation in the N-substituted oxo-cyclohexadienylidene porphyrinogen macrocycles. Such stability is an important factor when considering potential applications of these compounds.

The electron deficiency in **2**−**4** suggests that these materials can be considered as highly π-conjugated, sterically hindered quinones albeit connected via the tetrapyrrole moiety (by extension, this leads to the supposition that the reduced states of **2** (i.e., porphyrin, **1**, and its dication) can be labeled the conjugate hydroquinones). This conjecture helps to predict which further derivatives of the system represent worthwhile goals. However, while there are several synthetic variables available, the basic system presented here is still relatively undeveloped. The ability to bind metal ions (i.e., in **2** and **3**) and the availability of highly stable radical states are but two of the intrinsic features that make the N-alkylated *meso*-tetrakis(4-oxo-cyclohexadienylidene) porphyrinogens so appealing for further study.

Experimental Procedures

***meso*-Tetrakis-(3,5-di-*tert*-butyl-4-hydroxyphenyl)porphyrin, 1, and Its Two-Electron Oxidized Product, 2,** were prepared by modifications of previous procedures.[18] Respective yields were 17.5 and 95%. **1**: ^{1}H NMR (d_8-tetrahydrofuran): δ = 8.85 (8H, porphyrin pyrrolic β-H), 8.05 (8H, meso substituent H), 6.58 (4H, phenol OH), 1.63 (72H, *tert*-butyl-H), −2.62 (2H, br, porphyrin N−H) ppm. FAB-MS (3-NBA): m/z = 1127 $(M + H)^+$. UV−vis(1,2-dichlorobenzene) 428.5 (λ_{max}), 523.5, 562, 598, 655 nm. **2**: ^{1}H NMR (d_8-tetrahydrofuran): δ = 10.11 (br, pyrrolic N−H), 7.57 (8H, pyrrolic β-H), 6.87 (8H, meso substituent H), 1.33 (72H, *tert*-butyl) ppm. FAB-MS (3-NBA): m/z = 1127 $(M + 3H)^+$. UV−vis(1,2-dichlorobenzene): 350(sh), 517 (λ_{max}) nm.

3, N_{21},N_{23}-Dibenzyl-5,10,15,20-(3,5-di-*tert*-butyl-4-oxo-cyclohexa-2,5-dienylidene) Porphyrinogen and 4, N_{21},N_{22},N_{23},N_{24}-Tetrabenzyl-5,10,15,20-(3,5-di-*tert*-butyl-4-oxo-cyclohexa-2,5-dienylidene) Porphyrinogen. N-Alkylation of the oxidized porphyrin was performed in refluxing anhydrous ethanol/potassium carbonate with 5 equiv of benzyl bromide. **2** (200 mg, 1.8×10^{-4} mol) was dissolved in dry ethanol (20 mL), and anhydrous potassium carbonate (0.25 g) was added. The reaction mixture was stirred during the addition of benzyl bromide (150 mg, 8.8×10^{-4} mol, ∼5 equiv) followed by warming to reflux. Typically, the reaction was allowed to proceed until none of the parent porphyrinogen remained (tlc monitoring). Following completion of the reaction, the solvent was removed by evaporation under reduced pressure, and the resulting solid was partitioned between dichloromethane and water. Evaporation of the highly colored dichloromethane fraction yielded a green solid that was dissolved in the minimum of dichloromethane and chromatographed on silica gel eluting with *n*-hexane/dichloromethane, 1:1. The major products are consistently the di- and tetra-substituted products when benzyl bromide is used in the N-alkylation. The two main products are separated easily, but care must be taken to avoid contamination by the small amounts of trisubstituted derivative that are present in the mixture. Relative yields depend on reaction time, but the tetra-substituted product could be obtained in >80% yield if the reaction was allowed to proceed until virtually no disubstituted material, **3**, remained. The identity of the products was confirmed by ^{1}H NMR and FAB-MS.

3: ^{1}H NMR ($CDCl_3$): δ = 9.82 (br, NH), 7.57 (d, 4H, J = 2.44 Hz, pyrrolic β-H), 7.12 (m, 6H, benzyl ortho, para H), 7.00 (d, J = 2.44 Hz, 4H, pyrrolic β-H), 6.89 (d, J = 2.44 Hz, meso substituent alkene-H), 6.76 (dd, 4H, benzyl meta-H) 6.52 (s, 4H, meso-substituent alkene-H), 4.50 (s, 4H, benzyl CH_2), 1.33 (s, 36H, *tert*-butyl-H), 1.19 (s, 36H, *tert*-butyl-H) ppm. FAB-MS (3-NBA): m/z = 1308 amu $(M + 3H)^+$; UV−vis (1,2-dichlorobenzene): 333.0, 509 (λ_{max}) nm. **4**: ^{1}H NMR ($CDCl_3$): δ = 7.24 (s, obscured by $CHCl_3$, pyrrolic β-H), 7.16 (m, 12H, benzyl ortho, para protons) 6.67, 6.65 (m, 16H, benzyl meta-H (8H) + meso substituent alkene 8H), 4.52 (s, 8H, benzyl CH_2), 1.23 (s, 72H, *tert*-butyl groups) ppm. FAB-MS (3-NBA): m/z = 1486 amu $(M + 2H)^+$; UV−vis (1,2-dichlorobenzene): 331 and 504 (λ_{max}) nm.

Acknowledgment. The authors (Karlsruhe) thank the Deutsche Forschungsgemeinschaft (D.F.G.) for financial support. The authors are also thankful to the donors of the Petroleum Research Fund administered by the American Chemical Society and National Institutes of Health (F.D.) for support of this work.

Supporting Information Available: Additional experimental details. CIFs for **3** and **4**. Tables of crystallographic data including dihedral angles and displacements of atoms from the mean porphyrin planes for **3** and **4**. ORTEP and packing diagrams of **3** and **4**. Additional electronic absorption spectral data. Cartesian coordinates and projections of the calculated structures. This information is available free of charge via the Internet at http:// pubs.acs.org.

JO049401D